PERGAMON

Vision Research 39 (1999) 733–745

Vision Research

Evidence for the stochastic independence of the blue-yellow, red-green and luminance detection mechanisms revealed by subthreshold summation

Kathy T. Mullen *, Marcel J. Sankeralli

Department of Ophthalmology, McGill Vision Research, McGill University, 687 Pine Avenue West H4-14, Montreal H3A 1A1, Canada

Received 18 September 1997; received in revised form 9 February 1998

Abstract

We investigated the manner in which the outputs of the three postreceptoral mechanisms (red-green, blue-yellow and luminance) combine to determine contrast threshold. We used a subthreshold summation paradigm to test whether the combination of the postreceptoral mechanism outputs could be described by a probability summation model which assumes stochastic independence of the mechanisms, and determined the best fitting summation exponent. Stimuli were Gaussian enveloped 1 c/d sinusoidal gratings represented in a 3D cardinal space transformed from cone contrast axes, and normalized to detection threshold. The use of this space avoids the presence of elongated threshold contours, allowing a reliable model fit to include the less sensitive blue-yellow and luminance mechanisms. Our results were well fitted by the probability summation model and hence support the underlying stochastic independence of the three postreceptoral mechanisms.

Keywords: Color vision; Isoluminance; Red-green and blue-yellow mechanisms; Subthreshold summation

1. Introduction

The early stages of postreceptoral processing are believed to be subserved by three detection mechanisms, termed the red-green, blue-yellow and luminance mechanisms (Sperling & Harwerth, 1971; King-Smith & Carden, 1976; Kranda & King-Smith, 1979; Krauskopf, Williams & Heeley, 1982; Thornton & Pugh, 1983; Mullen & Kulikowski, 1990). The results of various studies suggest that the red-green mechanism linearly combines L- and M-cone outputs in balanced opposition, possibly with a small S-cone input, whereas the luminance mechanism, although more individually variable, sums L- and M-cones with the L-cones being more heavily weighted (Noorlander, Heuts & Koenderink, 1981; Stromeyer, Kronauer & Cole, 1983; Stromeyer, Cole & Kronauer, 1985; Cole, Hine & McIlhagga, 1993; Metha, Vingrys & Badcock, 1994; Stromeyer, Kronauer, Ryu, Chaparro & Eskew, 1995; Sankeralli & Mullen, 1996). Less is known about the blue-yellow mechanism since its cone contributions are harder to identify reliably using threshold contour methods (Noorlander, Heuts & Koenderink, 1981; Cole, Hine & McIlhagga, 1993; Sankeralli & Mullen, 1996), although the results of Sankeralli & Mullen (1996) indicate that the S-cones are in balanced opposition to the L- and M-cones. A different approach, involving a chromatic noise analysis, suggests the L- and M-cone weights are roughly equal in the blue-yellow mechanism (Sankeralli & Mullen, 1997).

This study explores the manner in which the responses of all three of the postreceptoral mechanisms are combined to yield a single neural response directly related to the detectability of a chromatic stimulus. It has frequently been assumed that the three postreceptoral mechanisms are independent and undergo a form of probability summation to determine threshold. In such probability summation, the net neural response R is the powered sum of the individual mechanism responses r (Quick, 1974):

* Corresponding author. Tel.: +1 514 8421231 ext 4757; fax: +1 514 843-1691; e-mail: kmullen@violet.vision.mcgill.ca

0042-6989/98/$ - see front matter
PII: S0042-6989(98)00137-0

$$R = \left\{ \sum r^k \right\}^{1/k} \quad (1)$$

where k is the summation exponent. This model describes the combination of the mechanism responses assuming stochastic independence (Graham, 1989). Such summation can account for the observed threshold contours in 2D color space, which resemble ellipses or parallelograms. The assumption of probability summation potentially provides the theoretical basis for the interpretation of threshold contours as revealing one mechanism as distinct from another, so allowing a single mechanism's cone weights to be assessed (Noorlander, Heuts & Koenderink, 1981; Stromeyer, Kronauer & Cole, 1983; Stromeyer, Cole & Kronauer, 1985). However, for reasons outlined below, only the combination of the responses of the red-green and luminance mechanisms have been extensively investigated, and even for these some controversy remains.

Several studies have successfully used a probability summation model to fit threshold contours in a cone contrast space spanning the red-green and luminance mechanisms (Cole, Hine & McIlhagga, 1993; Metha, Vingrys & Badcock, 1994; Sankeralli & Mullen, 1996). In another study, subthreshold summation was investigated under a range of spatial and temporal conditions (Mullen, Cropper & Losada, 1997). In this latter study, the summation exponent was estimated directly; the cone weights of the red-green and luminance mechanisms being predetermined from other data. These authors determined that a probability summation model provides a good description of this neural combination under a wide range of spatio-temporal conditions. Their results supported a probability summation model with a relatively high exponent ($k = 4$) and allowed the clear rejection of the linear model ($k = 1$). Their results, however, remain in conflict with a previous study (Gur & Akri, 1992) which reported a linear combination across a range of spatial frequencies.

The aims of the present study are 2-fold. Firstly, we specifically address the rules for the combination of the blue-yellow mechanism with the other two mechanisms (red-green and luminance), using a subthreshold summation paradigm. Existing threshold contour studies that have attempted to isolate the thresholds of the blue-yellow mechanism have typically produced highly elongated contours due to the insensitivity of the blue-yellow mechanism compared to the other two mechanisms in cone contrast space (Noorlander, Heuts & Koenderink, 1981; Cole, Hine & McIlhagga, 1993; Sankeralli & Mullen, 1996). For example, for a 1 c/d grating, a typical cone contrast threshold ratio for blue-yellow and red-green stimuli is 15:1, and for blue-yellow to luminance is 3:1 (Sankeralli & Mullen, 1996). This relative insensitivity of the blue-yellow mechanism severely limits the reliable fitting of the contour in the mechanism direction, and hence has impeded the determination of the cone weights of the blue-yellow mechanism and the comparison of different threshold contour models.

For these reasons, little is currently known about the form of the interactions between the blue-yellow mechanism and each of the other two. There is evidence for the existence of an independent blue-yellow mechanism from adaptation studies suggesting no cross adaptation between blue-yellow and red-green mechanisms (Krauskopf, Williams & Heeley, 1982), from measurements of chromatic discrimination (Krauskopf & Gegenfurtner, 1992), and from chromatic noise masking studies which indicate little masking of the blue-yellow mechanism by red-green noise, or vice versa (Sankeralli & Mullen, 1997). However, there have been no reliable tests for probability summation involving the blue-yellow mechanism as there have been for the interaction between the red-green and luminance mechanisms.

Secondly, it has been claimed (Wandell, 1985) that the interactions between the two chromatic mechanisms may differ fundamentally from interactions involving the luminance mechanism. Wandell (1985) reports that discrimination between two near-threshold stimuli that activate respectively a chromatic and luminance mechanism are 'categorical' in nature, requiring that, to be distinguishable, two stimuli must be drawn from either side of a perceptual boundary. By contrast, it is argued that color discriminations based solely on opponent color responses display no such categorical limitations. Whether or not this distinction is verified, the point remains that the mode of interaction between the red-green chromatic and luminance mechanisms, which has been extensively studied, cannot be assumed to extend to color–color interactions.

The main limitation to the measurement of subthreshold interactions with the blue-yellow mechanism has been the inappropriate choice of color space. In this study, thresholds are determined for combinations of the three detection mechanisms using a cardinal space. This space is a linear transformation of cone contrast coordinates with axes scaled in multiples of threshold. The scaling with threshold avoids the presence of elongated contours allowing an evenly spaced sampling of the contributing mechanisms and hence a more accurate fitting of a probability summation model.

In this paper, the estimate of k for the probability summation model of combination of the postreceptoral mechanisms serves two purposes. Firstly, it enables us to test for linear summation ($k = 1$) in which the combined response of the postreceptoral mechanisms is determined by the sum of the absolute values of the mechanism responses. Secondly, the estimation of k can be used to test for the degree of subthreshold interaction among the mechanisms. For example, Euclidean summation ($k = 2$) produces elliptical threshold contours in a 2D color space, whereas a higher k value

produces a more squared-off shape indicating less interaction, and for the highest k values there is a winner take all' combination with very little interaction among mechanisms.

2. Methods

2.1. Assumptions and the color space

We use a 3D color space defined by the cardinal directions of the three postreceptoral detection mechanisms. This space is a linear transformation of cone contrast space (Noorlander & Koenderink, 1983; Stromeyer, Cole & Kronauer, 1985; Cole, Hine & McIlhagga, 1993; Sankeralli & Mullen, 1997). Our cardinal space is similar to that adopted by Derrington, Krauskopf & Lennie (1984). However, it has the important difference that, as a linear transform of cone contrast space, its axes are independent of background chromaticity, assuming Weber adaptation of the cone responses (see Eskew, McLellan & Giulianini, 1999 for a review). The cardinal axes thus remain invariant with respect to their cone weights. We also assume that the postreceptoral mechanisms are the linear combination of the three cone types (L, M and S). This assumption is supported by heterochromatic additivity (Boynton & Kaiser, 1968; Guth & Graham, 1975), and measurements of detection threshold contours in a cone contrast space (Stromeyer, Cole & Kronauer, 1985; Cole, Hine & McIlhagga, 1993; Eskew, McLellan & Giulianini, 1999).

The axes of a cardinal space represent the stimulus directions which isolate the red-green, blue-yellow and luminance mechanisms, respectively. We select our cardinal directions directly from a knowledge of the cone weights of the three postreceptoral mechanisms provided by earlier studies using threshold contours (Sankeralli & Mullen, 1996) and noise masking (Sankeralli & Mullen, 1997). These studies identified a red-green mechanism consisting of equally weighted opponent L- and M-cone inputs (L-M), a blue-yellow mechanism of S-cones balanced by an equally weighted combination of L- and M-cones, and for two of the subjects, a luminance mechanism with an L to M-cone ratio of 2.75:1 (Sankeralli & Mullen, 1996). For the third subject (KTM) the cone weights of the luminance mechanism were assessed using a minimum motion task as described in Mullen, Cropper & Losada (1997). From these estimated mechanism directions, the cardinal direction was obtained as the unique direction orthogonal in cone contrast space to the vector directions representing the other two post receptoral mechanisms (Cole, Hine & McIlhagga, 1993). This definition is consistent with the assumption that each mechanism consists of a linear combination of cone responses. From the cone weights given above, the red-green cardinal axis was calculated to be in the L-3M-S direction (isoluminant and iso blue-yellow, adjusted for KTM according to the isoluminant point obtained in the minimum motion task), the blue-yellow cardinal axis was the S-cone direction (isoluminant and iso red-green) and the achromatic cardinal axis was in the $L+M+S$ direction (isochromatic) in (L, M, S) cone contrast space. Each cardinal axis was scaled individually for each subject using an initial measurement of contrast threshold.

2.2. Stimuli, apparatus, subjects and procedure

Stimuli were 1 c/d horizontal sinusoidal gratings windowed horizontally by 4° wide hard-edged vertical strip and vertically by a Gaussian envelope ($\sigma = 1.4°$). The grating was presented with a Gaussian temporal envelope ($\sigma = 188$ ms). The spatial and temporal average luminance and chromaticity of the stimulus was that of the white background. Stimuli were presented on a Barco calibrator CCID7651 RGB monitor (672×750 pixels; frame rate 75 Hz; line rate 60 kHz) driven by a Cambridge research systems VSG2/1 video controller interfaced with a Dell 333D computer. The monitor screen ($11 \times 11°$) was set near equal energy white (CIE (0.28, 0.30), 55 cd m^{-2}), and was viewed at 1.5 m. Each monitor phosphor was driven by a 14-bit digital-to-analog converter fed by a 12-bit look-up-table (LUT). The entries in the LUTs, used to linearize the phosphor output, were computed from a gamma fit to the voltage-to-irradiance characteristic of each phosphor, as measured using a united detector technology optometer (UDT S370) fitted with a radiometric detector (model 260). The software driving the LUTs computed the LUT inputs based on a second calibration measurement using a linear fit. The resulting contrast error in each phosphor was less than 0.017 log unit of contrast.

Results were obtained on three subjects, the two authors (MJS and KTM) and one naive observer (DMD), all having normal color vision (Farnsworth Munsell 100 hue test and The City University colour vision test).

Detection thresholds were measured using a two-alternative forced choice staircase procedure in which the test stimulus appeared in one of two 500 ms time intervals and the other interval was blank. The subject indicated by pressing a button in which interval the test stimulus appeared, and feedback was given after each trial. The step size of the staircase, -0.05 log unit following two consecutive correct responses and $+0.1$ log unit following an incorrect response, provided a threshold measurement at the 81.6% correct detection level. The threshold was determined in log units as the mean of the contrasts of the last six of eight reversals.

Each plotted threshold represents the mean of at least 3–4 measured thresholds. Threshold measurements were obtained using one of two experimental paradigms.

2.3. 'Fixed pedestal' paradigm

In this paradigm, thresholds were measured for a variable contrast test grating superimposed on a fixed contrast pedestal grating. The test and pedestal combination were presented in one interval and the other interval was blank. The test grating was from one cardinal axis, and the pedestal grating from another cardinal axis. In this procedure, both color angle and vector length vary from trial to trial. Test contrast thresholds were measured as a function of subthreshold pedestal contrast. The cardinal axes representing the dependent and independent variables were then switched to complete the 'summation square'. This was repeated for all six pairs of different cardinal axes and for both phases of test-pedestal superposition.

The use of a fixed subthreshold pedestal can restrict the sampling of the 'corners' of the summation square since, once the fixed pedestal contrast approaches its threshold value, it may become visible on some of its presentations and possibly interfering with the staircase methods, lowering the measured threshold. To avoid this problem, the pedestal was not presented at values close to threshold (not above 0.85 for MJS and DMD, and not above 0.80 for KTM), and if the pedestal ever became visible the measured test threshold was rejected and the pedestal contrast lowered. This is important as the estimated values of k depend critically on the corner values. As an additional precaution, we adopted a second paradigm, the 'fixed angle' paradigm, which does not require a fixed pedestal. This second paradigm is also more practical for the sampling of the color space in 3D.

2.4. 'Fixed angle' paradigm

This was used to measure 2D threshold contours and 3D surfaces in the color space. No pedestal was used. The direction of the test stimulus is fixed in the cardinal color space. The contrast threshold of the test stimulus was measured for a range of different directions: (i) in 12 directions for each of the three planes defined by the cardinal axes (*rg* and *lum*, *by* and *lum*, *rg* and *by*) (2D contours); and (ii) in 61 directions (including the 33 directions used for the 2D contours) in 3 cardinal space (3D contours). While this paradigm should yield the same threshold contour as the 'fixed pedestal' paradigm, it permits stimuli to be selected at all positions between the cardinal axes, including the corners of summation square which were avoided in the previous method.

2.5. Model

The model we test is one of probability summation of independent postreceptoral detection mechanisms. The model predicts how the likelihood of detection is greater when independent mechanism are stimulated together than when any mechanism is stimulated alone. The psychophysical effects of probability summation have been described thoroughly elsewhere (Sachs, Nachmias & Robson, 1971; Graham, Robson & Nachmias, 1978; Graham, 1989; Boynton, Ikeda & Stiles, 1964). In the Quick (1974) form of the probability summation model (the vector magnitude model), the psychometric function relating the combined output of the postreceptoral mechanisms to the probability of correctly detecting the stimulus can be obtained by assuming that each of the postreceptoral mechanisms has an associated Weibull probability of seeing function. These are then all combined as independent probability distributions. As Cole, Hine & McIlhagga (1993) show, the probability summation model predicts detection threshold contours given by:

$$\sum_i |\boldsymbol{m}_i \cdot \boldsymbol{p}|^k = 1 \tag{2}$$

where $\boldsymbol{m}_i$ is a 3D vector whose elements are the L-, M- and S-cone inputs of each of the three mechanisms in turn, and $\boldsymbol{p}$ is the 3D locus of the threshold contour in cone contrast space. In our cardinal space, this equation simplifies to:

$$rg^k + by^k + lum^k = 1 \tag{3}$$

where *rg*, *by* and *lum* represent the locus of the contour (Appendix A). The value of k determines the shape of the threshold surface. If $k = 1$, implying linear summation between mechanisms, the data would lie along a line joining the thresholds on the two cardinal axes, as indicated by the dashed lines in the figures. The presence of independent detection mechanisms combining to determine threshold by probability summation is revealed by a shape parameter greater than one. When $k = 2$ (Euclidean summation) the model yields a circular fit when placed in cardinal axes scaled in threshold multiples. When k is greater than two, the model yields a rounded square, and when k is very large ($\rightarrow \infty$), a perfect square whose face normals lie along the cardinal axes. The solid lines in the figures indicate the probability summation fits to our data.

As Quick (1974) shows, the parameter k is given by the slope of the probability of seeing functions of the postreceptoral mechanisms, assuming that these slopes are all similar. It is presently controversial whether there are significant differences among the slopes of the psychometric functions, as it is difficult to measure the psychometric slope with sufficient accuracy. Some studies find a steeper slope for the luminance mechanism

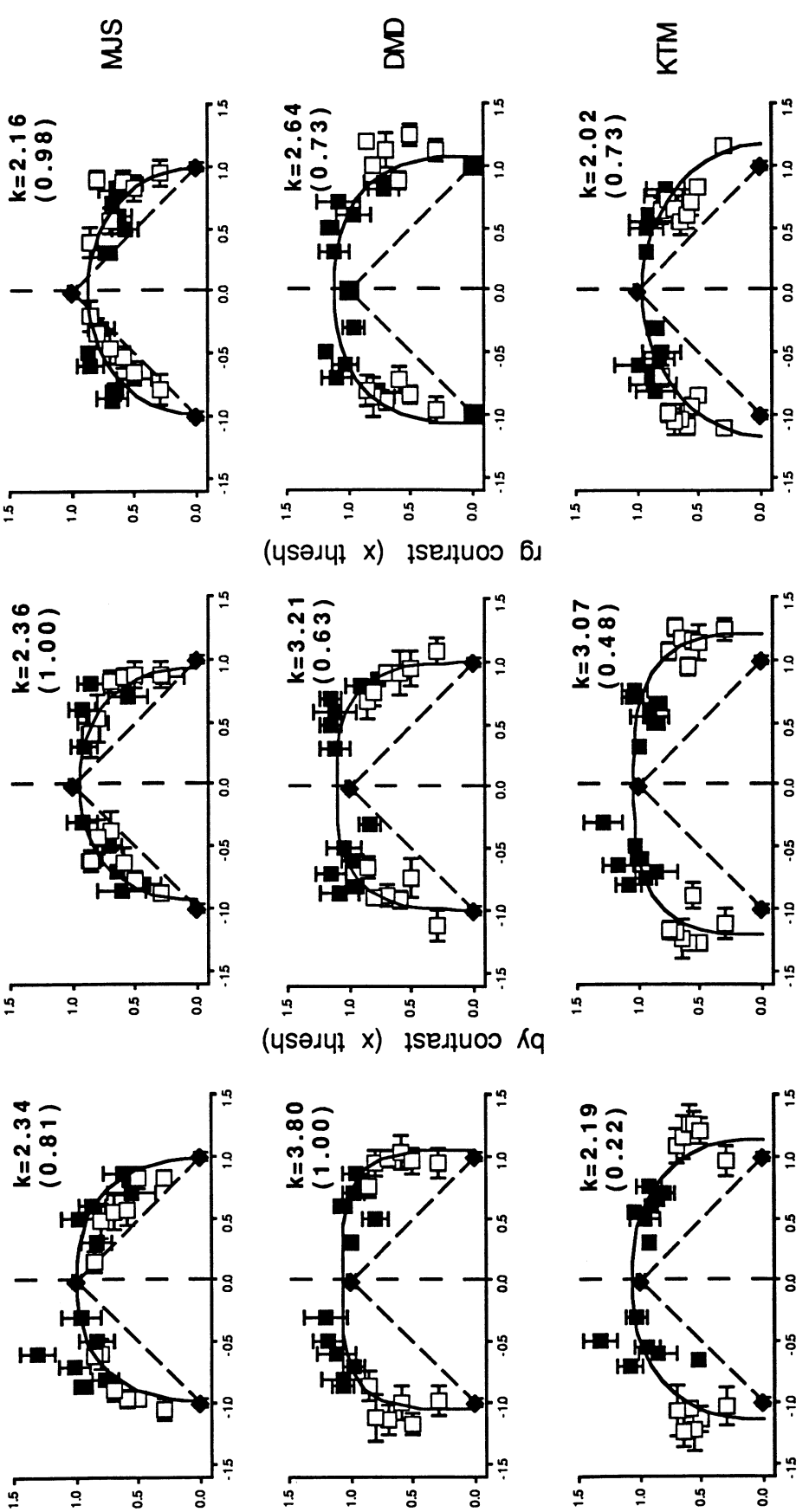

Fig. 1. Threshold contours for the 'fixed pedestal' paradigm arranged by subject (rows: MJS, DMD and KTM) and color plane (columns: *rg* with *lum*, *by* with *lum*, and *rg* with *by*). In each plot, contrast thresholds for the test stimulus were obtained as a function of pedestal contrast, both scaled in multiples of their respective detection thresholds when presented alone. Filled symbols represent test threshold on the vertical axis plotted against pedestal contrast on the horizontal axis. For the hollow symbols, the test and pedestal axes are reversed. The data set was fitted by a probability summation model (Eq. (4), solid curve). Fitted k values are shown on the plot with Q values in parentheses. The linear summation model is given by the dashed lines. '*rg*': red-green cardinal axis. '*by*': blue-yellow cardinal axis. '*lum*': achromatic cardinal axis. See Methods for the cone weights of the axes. Error bars show ± 1 S.E.

(Stromeyer, Lee & Eskew, 1992; Cole, Hine & McIlhagga, 1994), whereas others find no significant difference in psychometric slope across chromaticity (Maloney, 1990; Watanabe, Smith & Pokorny, 1997). Furthermore, based on the measurement of 160 psychometric functions over two subjects obtained as part of another study (Metha & Mullen, 1996), a significantly steeper slope for the luminance psychometric function was found for one of two subjects, but no differences were obtained between the slopes for the blue-yellow and red-green mechanisms. Given the tendency for any differences in the slopes of the chromatic and luminance mechanisms to disappear into the variability of the data, we conclude that the differences are relatively small, and for the purposes of our model we have assumed a constant slope across the three psychophysical detection mechanisms.

The equation was fitted to the data using a method of least χ^2 weighted by the inverse of the standard deviations of the data points. All standard deviations were converted from logarithmic to linear units. For the 'fixed pedestal' paradigm both axes can be independent variables and standard deviations were measured in either the horizontal or the vertical direction. For the fit, the averaged color and averaged luminance standard deviation were calculated for each summation contour. To determine the fit, these values were assumed to be applicable to the vector joining the origin of the figure and the data point. For the fixed angle method, standard deviations were obtained in the direction of the chromatic modulation. The goodness of fit is given by the χ^2 value, and the degrees of freedom, from which a Q value was calculated and shown on the figures. For the given degrees of freedom (d.f.), Q is a χ^2 distribution function which gives the probability that the minimum χ^2 is as large as it is purely by chance. In other words, for small Q values, the deviation from the model is unlikely to be due to chance and the model may be incorrect. For larger Q values, the deviation from the model is more likely to arise by chance suggesting the model is an adequate description of the data. A Q value of 0.1 or greater suggests an acceptable fit (Press, Teukolsky, Vetterling & Flannery, 1992).

3. Results

Results for the summation to threshold obtained using the 'fixed pedestal' paradigm for the three combinations of cardinal axes are shown for the three subjects in Fig. 1. Left, middle and right columns show one of the three planes defined by the cardinal axis pairs (*rg* and *lum*, *by* and *lum*, and *rg* and *by*, respectively). The right half of each plot represents one phase of combination of the grating pair, and the left half shows the reverse phase, as specified in the legend. Filled symbols with vertical error bars, indicate that the independent variable was along the horizontal axis, and hollow symbols with horizontal error bars indicate the reverse. For example, in the left hand column, hollow symbols represent the detection of luminance contrast in the presence of subthreshold red-green pedestal, and filled symbols represent the detection of red-green in the presence of a subthreshold luminance pedestal. All data points (both phases, filled and hollow symbols) were combined in order to make the fit. The error bars represent the standard error of the test contrast threshold measurement.

The solid curve shows the fit by least squares to the 2D form of Eq. (2):

$$(x/a_x)^k + (y/a_y)^k = 1 \tag{4}$$

where x and y depict the appropriate pair of stimulus coordinates (*rg*, *by* or *lum*). The fit parameters are a_x and a_y, which provide an estimate of the thresholds in the two cardinal axes and are therefore close to unity, and k is the value of interest. The fitted function is given by the solid line, and the fitted k value is marked on each panel along with its associated Q value.

The results for the fixed-angle paradigm are shown in Fig. 2. For each plot, detection thresholds were obtained in 12 directions in the planes defined by the same three cardinal axis pairs. We again fit the data to the probability summation model. Values of k are given on each panel. There is no significant difference between the k values obtained using the two different methods. For the data of Fig. 1 and Fig. 2, we have calculated and plotted the residuals of the fit. These showed no systematic deviations from the model fit, apart from small skews in individual plots (see Section 4).

Using the fixed angle method, we next measured threshold data along 61 axes spanning the cardinal space in 3D and fits were made to the probability summation model (Eq. (5)) using a least squares fit. In Eq. (5) we assume that k_{col} and k_{lum} are similar, differing by less tham a factor of 2.

$$\left[\left(\frac{rg}{a_{rg}}\right)^{k_{col}} + \left(\frac{by}{a_{by}}\right)^{k_{col}}\right]^{(k_{lum}/k_{col})} + \left(\frac{lum}{a_{lum}}\right)^{k_{lum}} = 1 \tag{5}$$

Individual fits were made within the isoluminant (*rg*-*by*) plane (k_{col}) represented as the horizontal plane in Fig. 3, and between the planes involving interactions with the luminance mechanism (k_{lum}) shown as the back plane (*rg* and *lum*) and the side plane (*by* and *lum*) in the figure. The fit parameters and the associated Q values are shown on the figures. As in the 2D case, the χ^2 values for the probability summation model show agreement between the model and the threshold data.

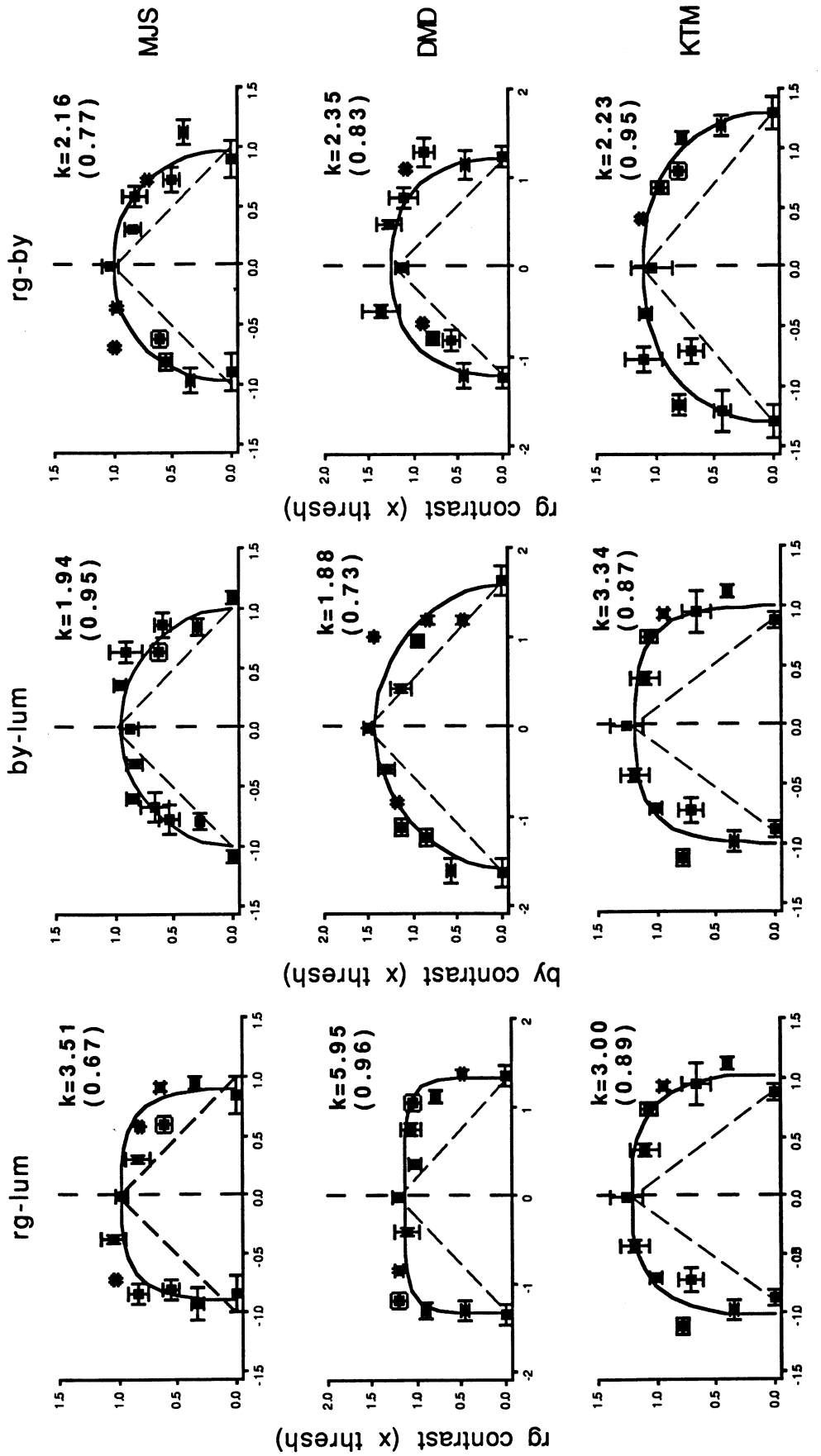

Fig. 2. Threshold contours for the 'constant ratio' paradigm arranged by subject (rows) and color plane (columns) as in Fig. 1. Each threshold measurement was made in the vector direction joining the data point to the origin. For the purposes of plotting, the standard error for each data point is resolved into the two axial directions (the measured standard errors is the root-sum-square of these two components). Other details as for Fig. 1.

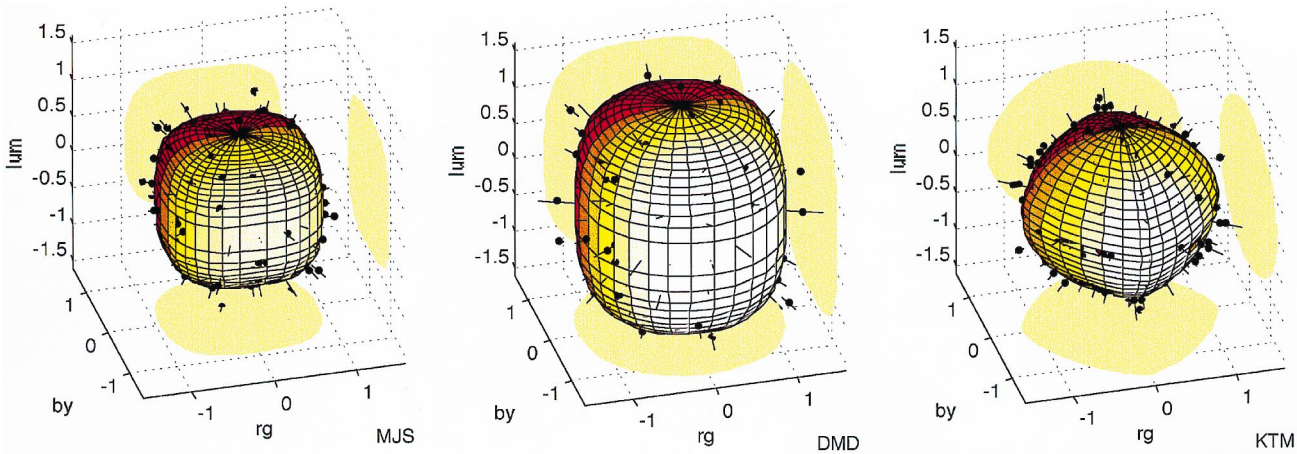

Fig. 3. The 3D threshold contours for the 'constant ratio' paradigm for three subjects (MJS, DMD and KTM). Each threshold measurement was made in the vector direction joining the data point to the origin. The data were fitted by a probability summation model (Eq. (5), meshed contour). Fitted k_{col}, k_{lum} values and associated Q values, respectively are 2.7, 3.61, Q = 1 (MJS); 2.17, 3.27, Q = 0.87 (DMD); 1.47, 1.88, Q = 1 (KTM). The flat shadowed areas represent the projection of the fitted contour on to each of the color planes. Data points lying internal to the solid are not visible, except where error bars project through the surface.

4. Discussion

Averaging across the three subjects and the two paradigms used in Figs. 1 and 2 the following average k values are obtained for each cardinal pair: $k = 3.50 \pm 1.30$ for the red-green and luminance axes, $k = 2.63 \pm 0.66$ for the blue-yellow and luminance axes and $k = 2.25 \pm 0.22$ for the red-green and blue-yellow axes. These values are all significantly greater than unity and hence are in agreement with the probability summation model as opposed to a linear summation model. This conclusion is supported by the data for the 3D fits shown in Fig. 3 for which similar results are obtained: the k value averaged across subjects for the combinations of the color and luminance mechanisms is 2.92 ± 0.92, and for the color-color pair is 2.11 ± 0.62. Our results thus support the assumption of stochastic independence of the three postreceptoral mechanisms. In particular, the present results show that the probability summation model can be extended to include interactions between the two color mechanisms (blue-yellow and red-green), and interactions between the blue-yellow and luminance mechanism. This is compatible with the functional independence of the three postreceptoral mechanisms, demonstrated by other approaches, including adaptation (Krauskopf, Williams & Heeley, 1982; Cole, Stromeyer & Kronauer, 1990), pattern masking (Gegenfurtner & Kiper, 1992; Mullen & Losada, 1994; Losada & Mullen, 1995) and noise masking (Poirson, Wandell, Varner & Brainard, 1990; Losada & Mullen, 1995; Sankeralli & Mullen, 1997).

4.1. Relationship to previous data

Previous threshold contour studies have generally most successfully investigated the interactions between the red-green and luminance mechanisms, and our results are in agreement with these in supporting probability summation between the red-green and luminance mechanisms (Kranda & King-Smith, 1979; Cole, Hine & McIlhagga, 1993, 1994; Metha, Vingrys & Badcock, 1994; Sankeralli & Mullen, 1996; Mullen, Cropper & Losada, 1997). Mullen, Cropper & Losada (1997) used a threshold normalized, cardinal color space with methods virtually identical to those used in Fig. 1 to examine interactions between the red-green and luminance mechanisms. They reported a best fitting probability summation model with an average k value of four, similar to the average value of 3.5 found here for red-green and luminance interactions. (The slightly higher k found in the previous study (Mullen, Cropper & Losada, 1997) may be due to the use of a bite-bar and headrest, which tends to stabilize fixation and attention).

Generally, the k values observed from earlier contour threshold methods fall in the range of 3–5(Kranda & King-Smith, 1979; Cole, Hine & McIlhagga, 1993, 1994; Metha, Vingrys & Badcock, 1994; Sankeralli & Mullen, 1996). Compared to these results, our estimates of k are somewhat lower (2.25–3.5). There are a number of possible reasons for this. Firstly, previous studies have been best able to fit red-green and luminance interactions and, as discussed below, these may genuinely have a higher summation exponent than the color-color interactions. Secondly, our lower estimates of k may be the more accurate estimates, resulting from our choice of color space. The more elongated contours obtained in other non-normalized color spaces and the concomitant poor sampling of the corners of the contours tend to bias the fitted k towards a high value. This can be seen by comparing our results with those of Sankeralli & Mullen (1996) who measure contours in

cone contrast space for two of the same subjects under the same spatio-temporal condition. Our results may, therefore, reflect a more accurate estimate of k from detection threshold contours. In support of this, we note that our k values are closer to the measured slopes of the psychometric functions for the detection of cardinal stimuli, which typically fall in the range of 2–3 (Maloney, 1990; Cole, Hine & McIlhagga, 1994) (see Section 4.2).

Thirdly, a possible source of error in our estimated values of k lies in the selection of the cardinal axis used to define our chosen color space. These cardinal axes were mainly derived empirically from estimates of the cone weights to the postreceptoral mechanisms obtained in an earlier study (Sankeralli & Mullen, 1996), although in one subject minimum motion estimates were used for the red-green cardinal direction. Errors in the selection of the cardinal directions would manifest themselves as an asymmetrical 'skewing' of the contours in cardinal space. We note, for instance, that the data for DMD in the *rg-by* condition of the fixed-angle paradigm exhibits some skewing to the right. By fitting a symmetrical contour to such data, there may be a systematic shift of estimated k values toward higher or lower values. To account for such possible inaccuracies in the cardinal axes, we performed an additional fit in which the directions of the axes were freely fitted. We applied this fit to four cases in which data skewing was apparent. Such a model did not improve the fit to skewed data, based on a χ^2 criterion. Furthermore, there was no systematic shift of the estimated k value when the skewed fit was applied. We therefore concluded that keeping our cardinal axes fixed at our chosen values provided the best achievable representation of the data. We note that the more rounded contours obtained with the blue-yellow cardinal direction may conceal possible skewing. However, the assessment of the blue-yellow cardinal direction (as for all the cardinal directions) is supported by other independent methods, including the assessment of the isoluminant plane using minimum flicker and the assessment of the cardinal directions using nulls in chromatic noise masking (Sankeralli & Mullen, 1997).

Our results are in conflict with a best fitting linear model for red-green and luminance interactions reported by Gur & Akri (1992). It should be noted that the good fit by $k=1$, as reported by Gur & Akri (1992), does not in itself exclude a probability summation model, since with such an exponent of unity the model reduces to $R=|rg|+|lum|$, and implies that the slopes of the psychometric functions are unity. However, this possible outcome is discounted by Gur & Akri (1992) on the basis that of their measured psychometric functions for the combination of red-green and luminance gratings which could not have been obtained from the stochastically independent combination of the psychometric functions of the individual red-green and luminance components. The reasons for the discrepancies between their linear model for red-green and luminance contrast combinations and other data supporting independent mechanisms remain unknown. Possibilities involving the intrusion of chromatic aberrations or the definition of color contrast used by Gur & Akri (1992) have already been considered and dismissed (Mullen, Cropper & Losada, 1997). A remaining candidate is possible errors in the measurement of the isoluminant point, which was established using very different spatial and temporal conditions from those used for test stimuli in the experiments.

4.2. Alternative interpretations of the Quick pooling formula

Our results are well fitted by the Quick pooling formula, and hence are compatible with the application of the probability summation model, and the assumption of the stochastic independence of the underlying detection mechanisms. Needless to say, our results cannot exclude alternative models producing the same fit to the data. Such alternatives include a deterministic combination of mechanism outputs, in which the outputs of the individual detectors are magnitudes, not probabilities. (For example, linear mechanism with non-linear pooling. or non-linear mechanisms with linear pooling, plus noise at a later stage) (see Graham, 1989 p. 169). The deterministic model, however, still reflects the underlying existence of separable detectors for the red-green, blue-yellow and luminance mechanisms. For this model, there is no expected relationship between the slopes of the psychometric functions and the amount of summation (k), whereas for the probability summation model these two values should be similar.

As already noted, it is curious that in the literature reported k values are sometimes higher than would be expected from the slopes of the psychometric functions for the individual cardinal mechanisms (Cole, Hine & McIlhagga, 1993), although for our data this difference is rather small. As noted above, a complete lack of an association would favor a deterministic interpretation of the data. On the other hand, it has been argued that a strong association does exist (Graham, 1989), and there are various explanations within the framework of a probability summation model for why the exponent and the slope of the psychometric function may not exactly match. Firstly, measured slopes will tend to be lower than their true value since they are measured over time, during which the actual threshold is likely to show variability. Secondly, the probability summation model incorporates both the high threshold assumption (that every 'correct' response by the observer reflects a detection by the underlying mechanisms and there are

no false positives) and the assumption of a Weibull fit to the probability functions. Neither of these assumptions are perfect (Graham, 1989) and their failings may alter the assessment of the amount of summation. Finally, and as discussed above, the determination of k depends critically on the data sampling the corner of the summation square. If such data are inadequate, as for example in the case of elongated contours, the value of k will be artificially high. In short, within the assumptions and limitations of the probability summation model, our data are compatible with the existence of stochastically independent red-green, blue-yellow and luminance detection mechanisms.

4.3. Interactions with the blue-yellow mechanism

The question arises whether our results demonstrate any differences between the red-green and luminance interactions and those involving the blue-yellow mechanism, or any differences between color-luminance interactions and color-color ones. The results of the present study are unclear with regard to this issue. For the 2D fits, the averaged k values are lower for the cardinal combinations that include the blue-yellow mechanism, and lowest for the color-color combinations. This same trend is reflected in the 3D data since the color-color combinations have a lower k than the color-luminance ones. A standard t-test on the averaged k values shows these effects not to be significant given the variability in the estimates. A paired t-test, however, which compares older-luminance and color–color summation exponents within each subject and condition, shows the former to be significantly greater than the latter ($P < 0.05$). We assume this reflects small differences in the slopes of the color and luminance psychometric fumctions.

Observations of the appearance of the test stimuli at threshold, suggest that there may be some underlying differences not revealed by a simple assessment of the summation exponent. When one of the chromatic mechanisms is paired with the luminance mechanism, the appearance of the stimuli at threshold makes a sharp transition between that of the cardinal chromatic stimulus and the achromatic stimulus as the stimulus direction is varied. This is reminiscent of the findings of Wandell (1985) who reported on the basis of near-threshold discrimination experiments that there is a categorical perceptual boundary between color and luminance stimuli, and of Mullen & Kulikowski (1990) who reported sharp transitions between the appearance of luminance based stimuli (lying in Sloan's notch) and stimuli detected by the red-green opponent mechanisms (lying on either side of the notch). On the other hand, when stimuli are restricted to the isoluminant plane the color appearance passed more gradually through several different stages. This is compatible with the data of Wandell (1985), implying that discriminations of near-threshold isoluminant stimuli have no categorical boundaries but are limited only by their separation in color space—a model which allows for a greater number of distinguishable colors in the isoluminant plane. Since these differences would imply a fundamental distinction in the way color-color and color-luminance mechanisms are combined to perform a discrimination task, further experiments on discrimination are required to follow-up these observations.

There has been recent theoretical interest in whether the value of the summation exponent is significantly greater than two, in the light of the 'Indeterminacy hypothesis' (Poirson, Wandell, Varner & Brainard, 1990; Knoblauch & Maloney, 1995). This hypothesis proposes that, for a summation exponent of two, a single elliptical threshold contour is not sufficient for the determination of the cone weights of the underlying postreceptoral mechanisms. This is because an exponent of two would produce a circular fit on our axes (or an ellipse in any linearly transformed axes), from which no unique set of 'privileged coordinates' can be derived. Instead, the directions of the postreceptoral mechanisms can only be derived from threshold contours grouped across an additional variable such as spatial frequency (Chaparro, Stromeyer, Kronauer & Eskew, 1994; Poirson & Wandell, 1996) or eccentricity (Stromeyer et al., 1992; Poirson et al., 1990), or from higher values of k from which the mechanism directions can be uniquely determined using a single threshold contour (Chaparro, Stromeyer, Kronauer & Eskew, 1994). As already discussed, there is quite extensive published data which demonstrates k values significantly above two for interactions between the red-green and luminance mechanism (Kranda & King-Smith, 1979; Cole, Hine & McIlhagga, 1993, 1994; Metha, Vingrys & Badcock, 1994; Sankeralli & Mullen, 1996; Mullen, Cropper & Losada, 1997). However, for interactions involving the blue-yellow mechanism, our data show an averaged k value quite close to two. To confirm whether an ellipsoidal fit could reasonably be applied to these data, we repeated all our model fits for Figs. 1 and 2 using a fixed k of two and from this we calculated new Q values. In most cases for interactions involving the blue-yellow mechanism, the Q values obtained by fixing $k = 2$ were similar to those obtained by fitting k freely. Results of a paired t-test using data from all subjects and conditions, however, showed that the fitted k values are significantly greater than 2 ($P < 0.05$), suggesting thst overall an elliptical fit to the data can be rejected. Although of theoretical interest, this conclusion has no impact on the interpretation of our results. Our cardinal axes are not fitted from the threshold contours reported here, but instead are predetermined and supported by a number of independent methods, including minimum flicker, noise masking, and the derivation of the mechanism directions from

sets of threshold contours spanning different spatio-temporal conditions (see Section 2).

4.4. Physiological significance

Neurophysiological recordings from the Macaque LGN have established that there are two distinct sub-populations of P cells drawing on either L- and M-cones alone or S-cones in combination with the L- and M-cones (Derrington, Krauskopf & Lennie, 1984). At the level of the primate cortex, there is evidence that these populations may become segregated into different 'blobs' in V1 (Ts'o & Gilbert, 1988), and this clustering may be retained, albeit more loosely, in the color ('thin') stripes of V2 (Roe & Ts'o, 1995). Thus there is physiological evidence to suggest that the red-green and blue-yellow psychophysical detection mechanisms are supported by different physiological subsystems. The finding of separable chromatic and luminance detection mechanisms is less easy to reconcile with the physiological data. The separation of the chromatic and luminance mechanisms cannot be attributed to detection on the basis of the P- and M-cell pathways, respectively, as the psychophysical independence of these two detection mechanisms is invariant with the spatial and temporal stimulus conditions, remaining even when P-cells determine both the color and luminance thresholds (Mullen, Cropper & Losada, 1997). It is thus likely that the P-cell responses are demultiplexed at a cortical level to form distinct color and luminance pathways (for possible models see Kingdom & Mullen, 1995). However, the physiological evidence for the location of such pathways remains tenuous as the majority of cortical neurons that respond to color also show significant responses to luminance contrast (Thorell, De Valois & Albrecht, 1984; Lennie, Krauskopf & Sclar, 1990).

5. Conclusions

Our results show that probability summation between the three postreceptoral mechanisms (red-green, blue-yellow and luminance) provides a good model for detection threshold data on the basis of chi-squared fits, and are thus compatible with the underlying stochastic independence of these three mechanisms. This supports the conclusion that the blue-yellow mechanism is an independent mechanism at detection threshold, and that its interactions with the red-green and luminance mechanisms are both similar to each other and to the interaction already observed between the red-green and luminance mechanisms. In addition, we find some evidence for differences in color-color interactions as compared to color-luminance ones.

Acknowledgements

We would like to thank Dr Frank Ferrie of the McGill Centre for Intelligent Machines for use of his fitting software. This study was funded by the Medical Research Council of Canada to K.T. Mullen (MT–10819).

Appendix A. The probability summation model in cardinal space

The probability summation contour in cone contrast space is given by:

$$\sum_{i=1,2,3} (\bar{\boldsymbol{m}}_i \cdot \bar{\boldsymbol{p}})^k = 1 \tag{6}$$

where $\boldsymbol{m}_i$ are the cone weights of the ith mechanism, and $\boldsymbol{p}$ is the locus of the contour. Putting $\boldsymbol{m}_i = [x_i, y_i, z_i]^T$ and $\boldsymbol{p} = [l, m, s]^T$, the term $\boldsymbol{m}_i \cdot \boldsymbol{p}$ can be written as:

$$\bar{\boldsymbol{m}}_i \cdot \bar{\boldsymbol{p}} = [x_i, y_i, z_i] \begin{bmatrix} l \\ m \\ s \end{bmatrix} \tag{7}$$

which can be re-written:

$$\bar{\boldsymbol{m}}_i \cdot \boldsymbol{p} = \bar{\boldsymbol{e}}_i \begin{bmatrix} x_1 & y_1 & z_1 \\ x_2 & y_2 & z_2 \\ x_3 & y_3 & z_3 \end{bmatrix} \begin{bmatrix} l \\ m \\ s \end{bmatrix} \tag{8}$$

where $\boldsymbol{e}_i$ is the row vector whose ith element is 1, the other elements being 0. Cardinal space coordinates (rg, by, lum) are defined by:

$$\begin{bmatrix} x_1 & y_1 & z_1 \\ x_2 & y_2 & z_2 \\ x_3 & y_3 & z_3 \end{bmatrix} \begin{bmatrix} l \\ m \\ s \end{bmatrix} = \begin{bmatrix} rg \\ by \\ lum \end{bmatrix} \tag{9}$$

since the $[l, m, s]$ cone contrast vector in a cardinal direction at threshold yields a postreceptoral response (the sum weighted by the cone weights) equal to one for that cardinal coordinate and zero for all others. Substituting that into the previous equation yields:

$$\bar{\boldsymbol{m}}_i \cdot \bar{\boldsymbol{p}} = \bar{\boldsymbol{e}}_i \begin{bmatrix} rg \\ by \\ lum \end{bmatrix} \tag{10}$$

and the probability summation contour becomes:

$$\sum \left(\bar{\boldsymbol{e}}_i \begin{bmatrix} rg \\ by \\ lum \end{bmatrix} \right)^k = 1 \tag{11}$$

which, using the definition for e_i, gives:

$$rg^k + by^k + lum^k = 1 \quad (12)$$

which is the model used to fit the cardinal coordinate data.

References

Boynton, Ikeda & Stiles, 1964.

Boynton, R. M., & Kaiser, P. K. (1968). Vision: The additivity law made to work for heterochromatic photometry with bipartite fields. *Science*, *161*, 366–368.

Chaparro, A., Stromeyer, C. F., Kronauer, R. E., & Eskew, R. T. (1994). Separable red-green and luminance detectors for small flashes. *Vision Research*, *34*, 751–762.

Cole, G. R., Hine, T., & McIlhagga, W. H. (1993). Detection mechanisms in L-, M-, and S-cone contrast space. *Jorunal of the Optical Society ofAmerica A*, *10*, 38–51.

Cole, G. R., Hine, T. J., & McIlhagga, W. H. (1994). Estimation of linear detection mechanisms for stimuli of medium spatial frequency. *Vision Research*, *34*, 1267–1278.

Cole, G. R., Stromeyer, C. F., & Kronauer, R. E. (1990). Visual interactions with luminance and chromatic stimuli. *Journal of the Optical Society of America A*, *7*, 128–140.

Derrington, A. M., Krauskopf, J., & Lennie, P. (1984). Chromatic mechanisms in lateral geniculate nucleus of macaque. *Journal of Physiology*, *357*, 241–265.

Eskew, R.T., McLellan, J.S., Giulianini, F. Chromatic detection and discrimination: a theoretical review, in colour vision. In K. Gegenfurtner, L.T. Sharp (Eds.), *Molecular genetics to perception*. Cambridge University, Cambridge (in press).

Gegenfurtner, K. R., & Kiper, D. C. (1992). Contrast detection in luminance and chromatic noise. *Journal of the Optical Society of America A*, *9*, 1880–1888.

Graham, N.V.S. (1989). *Visual pattern analyzerse*. Oxford University, New York.

Graham, N. V. S., Robson, J. G., & Nachmias, J. (1978). Grating summation in fovea and periphery. *Vision Research*, *18*, 815–825.

Gur, M., & Akri, V. (1992). Isoluminant stimuli may not expose the full contribution of color to visual functioning: spatial contrast sensitivity measurements indicate interaction between color and luminance processing. *Vision Research*, *32*, 1253–1262.

Guth, S. L., & Graham, B. V. (1975). Heterochromatic additivity and the acuity response. *Vision Research*, *15*, 317–319.

Kingdom, F. A. A., & Mullen, K. T. (1995). Separating colour and luminance information in the visual system. *Spatial Vision*, *9*, 191–219.

King-Smith, P. E., & Carden, D. (1976). Luminance and opponent colour contributions to visual detection and adaptation and to spatial and temporal integration. *Journal of the Optical Society of America*, *66*, 709–717.

Knoblauch, K., & Maloney, L. T. (1995). Testing the indeterminacy of linear color mechanisms from color discrimination data. *Vision Research*, *36*, 295–306.

Kranda, K., & King-Smith, P. E. (1979). Detection of coloured stimuli by independent linear systems. *Vision Research*, *19*, 733–745.

Krauskopf, J., & Gegenfurtner, K. R. (1992). Color discrimination and adaptation. *Vision Research*, *32*, 2165–2175.

Krauskopf, J., Williams, D. R., & Heeley, D. W. (1982). Cardinal directions of colour space. *Vision Research*, *22*, 1123–1131.

Lennie, P., Krauskopf, J., & Sclar, G. (1990). Chromatic mechanisms in striate cortex of macaque. *Journal of Neuroscience*, *10*, 649–669.

Losada, M. A., & Mullen, K. T. (1995). Color and luminance spatial tuning estimated by noise masking in the absence of off-frequency looking. *Journal of the Optical Society of America A*, *12*, 250–260.

Maloney, L. T. (1990). The slope of the psychometric function at different wavelengths. *Vision Research*, *30*, 129–136.

Metha, A. B., & Mullen, K. T. (1996). Temporal mechanisms underlying flicker detection and identification for red-green and achromatic stimuli. *Journal of the Optical Society of Americas A*, *13*, 1969–1980.

Metha, A. B., Vingrys, A. J., & Badcock, D. R. (1994). Detection and discrimination of moving stimuli: the effects of color, luminance and eccentricity. *Journal of the Optical Society of America A*, *11*, 1697–1709.

Mullen, K. T., & Kulikowski, J. J. (1990). Wavelength discrimination at detection threshold. *Journal of the Optiacal Society of America A*, *7*, 733–742.

Mullen, K. T., & Losada, M. A. (1994). Evidence for separate pathways for color and luminance detection mechanisms. *Journal of the Optical Society of America A*, *11*, 3136–3151.

Mullen, K. T., Cropper, S. J., & Losada, M. A. (1997). Absence of linear subthreshold summation between red–green and luminance mechanisms over a wide range of spatio-temporal conditions. *Vision Research*, *37*, 1157–1165.

Noorlander, C., & Koenderink, J. J. (1983). Spatial and temporal discrimination ellipsoids in color space. *Journal of the Optical Societyof America*, *73*, 1533–1543.

Noorlander, C., Heuts, M. J. G., & Koenderink, J. J. (1981). Sensitivity to spatio-temporal combined luminance and chromaticity contrast. *Journal of the Optical Society of America*, *71*, 453–459.

Poirson, A. B., & Wandell, B. A. (1996). Pattern-color separable pathways predict sensitivity to simple colored patterns. *Vision Research*, *36*, 515–526.

Poirson, A. B., Wandell, B. A., Varner, D. C., & Brainard, D. H. (1990). Surface characterization of color thresholds. *Journal of the Optical Society of America A*, *7*, 783–789.

Press, W.H., Teukolsky, S.A., Vetterling, W.T., Flannery, B.P. (1992). *Numerical recipes in C: the art of scientific computing* (2nd ed.). Cambridge University, Cambridge.

Quick, R. F. (1974). A vector magnitude model of contrast detection. *Kybernetic*, *16*, 65–67.

Roe, A. W., & Ts'o, D. Y. (1995). Visual topography in primate V2: multiple representation across functional stripes. *Journal of Neuroscience*, *15*, 3689–3715.

Sachs, M. D., Nachmias, J., & Robson, J. G. (1971). Spatial frequency selective channels in human vision. *Journal of the Optical Society of America*, *61*, 1176–1186.

Sankeralli, M. J., & Mullen, K. T. (1997). Postreceptoral chromatic detection mechanisms revealed by noise masking in three-dimensional cone contrast space. *Journal of the Optical Society of America A*, *14*, 2633–2646.

Sankeralli, M. J., & Mullen, K. T. (1996). Estimation of the L-, M- and S-cone weights of the post-receptoral detection mechanisms. *Journal of the Optical Society of America A*, *13*, 906–915.

Sperling, H. G., & Harwerth, R. S. (1971). Red-green cone interactions in the increment threshold spectral sensitivity of primates. *Science*, *172*, 180–184.

Stromeyer, C. F., Cole, G. R., & Kronauer, R. E. (1985). Second-site adaptation in the red-green chromatic pathways. *Vision Research*, *25*, 219–237.

Stromeyer, C.F., Kronauer, R.E., Cole, G.R. (1983). Adaptive mechanisms controlling sensitivity to red-green chromatic flashes, in colour vision. In: J.D. Mollon, L.T. Sharpe, *Physiology and psychophysics* (pp. 313–330). Academic, London.

Stromeyer, C. F., Kronauer, R. E., Ryu, A., Chaparro, A., & Eskew, R. T. (1995). Contributions of human long-wave and middle-wave cones to motion detection. *Journal of Physiology*, *485*, 221–243.

Stromeyer, C. F. III, Lee, J., & Eskew, R. T. Jr. (1992). Peripheral chromatic sensitivity for flashes: A post-receptoral red-green asymmetry. *Vision Research*, *32*, 1865–1873.

Thorell, L. G., De Valois, R. L., & Albrecht, D. G. (1984). Spatial mapping of monkey V1 cells with pure color and luminance stimuli. *Vision Research*, *24*, 751–769.

Thornton, J. E., & Pugh, E. N. (1983). Red-green color opponency at detection thresholds. *Science*, *219*, 191–193.

Ts'o, D. Y., & Gilbert, C. D. (1988). The organization of chromatic and spatial interactions in the primate striate cortex. *Journal of Neuroscience*, *8*, 1712–1727.

Wandell, B. A. (1985). Color measurement and discrimination. *Journal of the Optical Society of America A*, *2*, 62–71.

Watanabe, A., Smith, V.C., Pokorny, J. (1997). Psychometric functions for chromatic discriminations. In C.R. Cavonius, *Colour vision deficiencies XIII*. Dordrecht, Kluwer Academic.